

University of Groningen

## Pyrolysis oil upgrading to transportation fuels by catalytic hydrotreatment

Wildschut, Jelle

**IMPORTANT NOTE: You are advised to consult the publisher's version (publisher's PDF) if you wish to cite from it. Please check the document version below.**

*Document Version*

Publisher's PDF, also known as Version of record

*Publication date:*

2009

[Link to publication in University of Groningen/UMCG research database](#)

*Citation for published version (APA):*

Wildschut, J. (2009). *Pyrolysis oil upgrading to transportation fuels by catalytic hydrotreatment*. s.n.

### Copyright

Other than for strictly personal use, it is not permitted to download or to forward/distribute the text or part of it without the consent of the author(s) and/or copyright holder(s), unless the work is under an open content license (like Creative Commons).

### Take-down policy

If you believe that this document breaches copyright please contact us providing details, and we will remove access to the work immediately and investigate your claim.

*Downloaded from the University of Groningen/UMCG research database (Pure): <http://www.rug.nl/research/portal>. For technical reasons the number of authors shown on this cover page is limited to 10 maximum.*

## Chapter 2: Hydrotreatment of Fast Pyrolysis oil using Heterogeneous Noble Metal Catalysts

### Abstract

Fast pyrolysis oils from lignocellulosic biomass are promising second generation biofuels. Unfortunately, the application range for such oils is limited due to the high acidity (pH ~ 2.5) and the presence of oxygen in a variety of chemical functionalities. Upgrading of the oil is required for most applications. We here report an experimental study on the upgrading of fast pyrolysis oil by catalytic hydrotreatment. A variety of heterogeneous noble metal catalysts have been tested for this purpose (Ru/C, Ru/TiO<sub>2</sub>, Ru/Al<sub>2</sub>O<sub>3</sub>, Pt/C and Pd/C) and the results are compared to typical hydrotreatment catalysts (sulphided NiMo/Al<sub>2</sub>O<sub>3</sub> and CoMo/Al<sub>2</sub>O<sub>3</sub>). The reactions were carried out at temperatures in the range of 250 to 350 °C and hydrogen pressures between 100 and 200 bar. The Ru/C catalyst appears superior to the classical hydrotreating catalysts with respect to oil yield (up to 60 %-wt.) and deoxygenation level (up to 90 %-wt.). The upgraded products were less acidic and contained less water than the original fast pyrolysis oil. The HHV was about 40 MJ/kg, which is about twice the value of pyrolysis oil. Analyses of the products by <sup>1</sup>H-NMR and 2D-GC showed that the upgraded pyrolysis oil contained less organic acids, aldehydes, ketones and ethers than the feed whereas the amounts of phenolics, aromatics and alkanes were considerably higher.

## **1. Introduction**

Increasing oil prices due to higher demand and less accessible resources have boosted the research activities in the field of renewable energy carriers. An interesting second generation bio-liquid is pyrolysis oil, obtainable from lignocellulosic biomass by flash pyrolysis in yields up to 70 %-wt. The oil is produced on demonstration- and semi-commercial scale by a number of companies [1]. The oil has a higher water and oxygen content than fossil oil, resulting in a lower energy density (15-19 MJ/kg) [1] compared to fossil oil (40 MJ/kg). Furthermore, the oil ages and tends to phase separate upon prolonged storage. As a consequence, the oil is not suitable for direct application in (instationary) internal combustion engines and requires upgrading to fulfill the stringent specifications for (bio-) fuels.

One of the upgrading technologies is catalytic hydrotreatment. Typically, harsh conditions (200-400 °C and 100-200 bar hydrogen pressure) are required to obtain reasonable volumetric production rates [2-5]. During such a hydrotreatment process multiple reactions occur like hydrogenation, hydrogenolysis, hydrodeoxygenation, decarboxylation, decarbonylation, cracking/hydrocracking and polymerization reactions leading to the formation of coke.

For a state of the art review on fast pyrolysis oil hydrotreatment the reader is referred to Elliot in 2007 [6]. An overview of work relevant for the present purpose is summarized in Table 1. Research activities on the HDO of pyrolysis oil started already in 1984 with the pioneering work of Elliot *et al.*[7]. Reaction conditions, catalysts and reactor systems were adopted from typical hydrotreating processes for fossil resources like hydrodesulphurization (HDS). Typically, trickle bed reactors (packed beds with down flow operation of both liquid and gas) were applied in combination with common HDS catalysts like sulphided NiMo/Al<sub>2</sub>O<sub>3</sub> and CoMo/Al<sub>2</sub>O<sub>3</sub>. To promote hydrogenation, Elliot *et al.* proposed a two stage reactor configuration. A first reactor is operated below 280 °C using a pressure of typically 140 bar and a LHSV (vol. oil/vol. cat.h) of 0.62 to ‘stabilise’ the oil by hydrotreating the most reactive compounds. A subsequent deep deoxygenation step was performed in a second reactor at higher temperatures, typically 350 °C, under hydrogen at a total pressure of 142 bar and a LHSV of 0.11 vol. oil/vol. cat.h. Continuous operation resulted in oil yields between 30-55 % and deoxygenation levels up to 99 %

[8,9]. Most studies were performed in continuous mode and only a few experimental studies in batch reactors have been reported [5,10,11,13]. The most likely reason for experimentation in continuous reactors is the anticipated strong resemblance between HDO and the well established HDS processing in continuous (packed bed) reactors.

Table 1. Summary of the research on HDO of pyrolysis oil.

Year	Authors (ref.)	Yield (%-wt.)	Deoxygenation (%-wt)	Reactor		Catalyst	Temperature (°C)	Pressure (bar)
				Type	Size (L)			
1984	Elliot, Baker [7]	80	90-95	Bench scale continuous flow reactor	1	NiMo and CoMo on Al <sub>2</sub> O <sub>3</sub>	350-450	138
1988	Gagnon, Kaliagiune[10]	n.r.	75	Batch slurry reactor	n.r.	first 5 %-wt. Ru/Al <sub>2</sub> O <sub>3</sub> and then NiO-WO <sub>3</sub> /Al <sub>2</sub> O <sub>3</sub> , CuCr	80-325	41-172
1988	Sheu, Anthony, Soltes [12]	n.r.	10-50	Trickle bed	0.157	Pt/Al <sub>2</sub> O <sub>3</sub> /SiO <sub>2</sub> ; sulphided CoMo, NiW& NiMo	350-400	53-104
1988	Elliott [2]	n.r.		Upflow packed bed	1	CoMo/Al <sub>2</sub> O <sub>3</sub>	stage 1:274; stage 2: 350-450	69-208
1992	Oasmaa [13]	65	86	Batch	n.r.	10%-wt. CoO/Al <sub>2</sub> O <sub>3</sub>	390	215
1994	Baldauf, Balfanz, Rupp [8]	30-35	88-99.9	Packed bed, up- and downflow	0.716	CoMo, NiMo sulphided	350-370	up to 300
			78-85	Slurry reactor	3-12			
1995	Conti, Scano, Baufola, Mascia [14]	72	60	2 Stage packed bed upflow	0.1- 1	NiMo sulphided	stage 1:140, stage 2:250-	50

							275	
1998	Samolada, Baldauf, Vasalols [15]	30-55	88-99.9	Packed bed, up- and downflow	0.8	NiMo, CoMo	Up to 500	Up to 325
1996-2004	Elliott, Neuen-schwander [16,17]	n.r.	31-99	2 Stage trickle bed	0.1; 0.425	NiMo, CoMo, sulphided; Ru/C and Ru/TiO <sub>2</sub>	150-390	75-150
2003	Su-Ping [5]	n.r.	90%	Batch slurry reactor	0.5	CoMo sulphided	360-390	15-30 (20 °C)

A serious issue in catalytic hydrodeoxygenation appears catalyst deactivation due to thermally induced polymerization and the formation of coke [15,18,19]. Coke deposit on the catalyst was shown to occur particularly with catalysts based on an alumina support [18,19].

We here report a systematic catalyst screening study in a batch reactor set-up. A variety of catalysts was screened for the hydrotreatment of raw pyrolysis oil at two operating conditions relevant for the HDO process i.e. at 250 °C and 100 bar to represent mild HDO and at 350 °C and 200 bar to represent deep HDO. This approach allows selection of the optimum catalyst for each of the steps with respect to oil yield and deoxygenation level. The second part of the chapter focuses on the properties and composition of the upgraded oils by a variety of analytical techniques.

## 2. Materials and Methods

### 2.1 Materials

The noble metal catalysts (Ru/ $\gamma$ -Al<sub>2</sub>O<sub>3</sub>, Ru/C, Ru/TiO<sub>2</sub>, Pd/C, Pt/C) were obtained as powders from Sigma Aldrich (all except Ru/TiO<sub>2</sub>) and Degussa (Ru/TiO<sub>2</sub>) and contained 5 %-wt. of active metal. Relevant properties of the catalysts were determined experimentally and the results are shown in Table 2. Pre-sulfided NiMo/ $\gamma$ -Al<sub>2</sub>O<sub>3</sub> and CoMo/ $\gamma$ -Al<sub>2</sub>O<sub>3</sub> were obtained from an anonymous supplier. No external sulphur source was added before/during the hydrotreatment reaction. Fast pyrolysis oil was supplied by BTG (Enschede) and was prepared from beech wood. The oil was filtered after

preparation and stored at  $-8^{\circ}\text{C}$  to avoid aging resulting in the formation of solids. Relevant data are given in Table 3. Hydrogen and helium were from Hoek Loos (Schiedam) and were of analytical grade (hydrogen 6.0). Nitrogen (technical grade,  $>98\%$  purity) was also obtained from Hoek Loos (Schiedam). Tetrahydrofuran and n-decane were obtained from Acros and were of analytical grade (99.99 %).

Table 2. Catalyst details

Catalyst	Supplier (cat. Number)	Dispersion (%)	Specific area ( $\text{m}^2/\text{g}$ )
Ru/ $\gamma\text{-Al}_2\text{O}_3$	Sigma Aldrich (84032)	22	186
Ru/C	Sigma Aldrich (206180)	11	886
Ru/ $\text{TiO}_2$	Degussa (31299457/2006)	18	55
Pd/C	Sigma Aldrich (20568)	16	1094
Pt/C	Sigma Aldrich (205931)	16	1155

### 2.2 Hydrodeoxygenation experiments

Fast pyrolysis oil was hydrotreated in a 100 ml batch autoclave setup (Buchi AG). The maximum pressure and temperature of the set-up are 350 bar and  $450^{\circ}\text{C}$ , respectively. The temperature of the system is controlled using an electric heating mantle combined with a cooling spiral using water. The reactor content was stirred at 1300 rpm with a magnetically driven gas inducing impeller. The impeller was of the Ruston type with four blades (d: 24 mm, h: 12 mm and 5.5 mm thickness). Temperature and pressure in the reactor vessel are measured and monitored by a PC. A schematic representation of the set-up is given in Figure 1.

The reactor was filled with fast pyrolysis oil (25 g) and catalyst (1.25 g, 5 %-wt. on basis of wet pyrolysis oil). Subsequently, the reactor was flushed with nitrogen gas and pressurized with 20 bar of hydrogen at room temperature. The reactor was heated to the intended reaction temperature (250 or  $350^{\circ}\text{C}$ ) with a heating rate of  $16^{\circ}\text{C}/\text{min}$  and kept at that temperature for the intended reaction time. The pressure in the reactor was set to the pre-determined value. The pressure during a run was kept constant by continuous feeding of hydrogen. After completion of the reaction, typically 4 h, the reactor was cooled to ambient temperature.

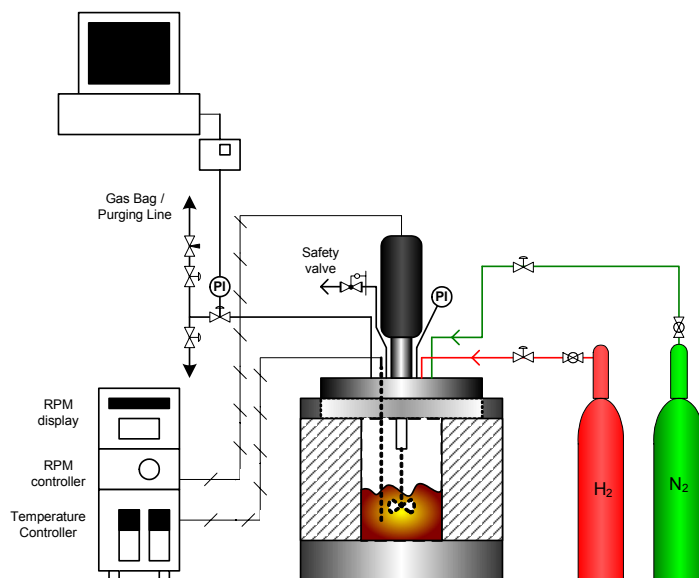


Figure 1. Schematic representation of the autoclave setup.

The pressure was recorded for mass balance calculations and the gas phase was sampled using a gas bag. The liquid product, consisting of a water phase and, depending on the catalyst and reaction temperature, one or two organic phases, was recovered from the reactor using a syringe and the liquid product was weighed. Subsequently, the reactor was rinsed with acetone. The combined acetone fractions with suspended solids were filtered. After filtration, the filter was dried and weighed. The amount of solids minus the original catalyst intake was taken as the amount of solids formed during the HDO process. The deep HDO experiments were conducted in duplicate. The mild HDO experiment with Ru/TiO<sub>2</sub> was conducted in duplicate, the remaining experiments were conducted once.

### 2.3 Analyses of the HDO oils

#### 2.3.1 GC/MS and 2D-GC analyses

Samples were either injected pure or diluted with tetrahydrofuran (THF) to 50 %-wt. n-decane was used as an internal standard.

GC-MS analysis were performed on a Quadrupole Hewlett Packard 5972 MSD attached to a Hewlett Packard 5890 GC equipped with a 30 m x 0.25 mm i.d. and 0.25  $\mu$ m film sol-gel capillary column. The injector temperature was set at 250 °C. The oven

temperature was kept at 40 °C for 5 minutes then heated up to 250 °C at a rate of 3 °C min<sup>-1</sup> and then held at 250 °C for 10 minutes.

2D-GC analyses were performed on a trace 2D-GC from Interscience equipped with a cryogenic trap system and two columns, a 30 m x 0.25 mm i.d. and 0.25 µm film of sol-gel capillary column connected to a 148 cm x 0.1 mm i.d. and 0.1 µm film Restek 1701 column. An FID detector was applied. A dual jet modulator was applied using carbon dioxide to trap the samples. The lowest possible operating temperature for the coldtrap is 60 °C. Helium was used as the carrier gas (flow 0.6 ml/min). The injector temperature and FID temperature were set at 250 °C. The oven temperature was kept at 60 °C for 5 minutes then heated up to 250 °C at a rate of 3 °C min<sup>-1</sup>. The pressure was set at 0.7 bar. The modulation time was 6 s.

### 2.3.2 Elemental composition, higher heating value (HHV), water content, flashpoint, viscosity and NMR analyses

The elemental composition of the HDO oils (C, H and N) was determined using an Euro Vector 3400 CHN-S analyzer. The oxygen content was determined by difference. The HHV of the samples was calculated using Milne's formula (eq. 1) [20]. Where C, H and O stands for carbon, hydrogen and oxygen in %-wt.

$$\text{HHV} = 338.2 \times C + 1442.8 \times \left( H - \frac{O}{8} \right) \text{ [MJ/kg]} \quad (\text{eq. 1})$$

The water content in the samples was determined by a Karl Fischer titration using an Metrohm Titrino 758 titration device. A small amount of product (0.03-0.05 g) was added to an isolated glass chamber containing Hydranal (Karl Fischer Solvent, Riedel de Haen). The titrations were carried out using the Karl Fischer titrant Composit 5K (Riedel de Haen). All measurements were performed in duplicate.

Flashpoints were determined using a Grabner Instruments mini flashpoint analyser with a temperature increase of 5.5 °C/min in the range of 30-80 °C.

The viscosity of the oil and products were determined with a AR 1000-N Rheometer from TA instruments. The temperature was set at 40 °C with a shear rate of 0.1 s<sup>-1</sup>. Each sample was measured 10 minutes to get an accurate constant value for the viscosity.

<sup>1</sup>H- NMR spectra were recorded on a 500 MHz NMR (Varian). The samples were dissolved in CDCl<sub>3</sub>.

#### 2.4 Gas phase analyses

The gas phases after reaction were collected and stored in a gasbag (SKC Tedlar 3 Liter Sample Bag (9.5" x 10")) equipped with a polypropylene septum fitting. GC-TCD analyses were performed on a Hewlett Packard 5890 Series II GC equipped with a Porablot Q Al<sub>2</sub>O<sub>3</sub>/Na<sub>2</sub>SO<sub>4</sub> column and a Molecular Sieve (5A) column. The injector temperature was set at 150 °C, the detector temperature at 90 °C. The oven temperature was kept at 40 °C for 2 minute then heated up to 90 °C at 20 °C/min and kept at this temperature for 2 minutes. The columns were flushed for 30 seconds with gas sample before starting the measurement. A reference gas containing H<sub>2</sub>, CH<sub>4</sub>, CO, CO<sub>2</sub>, ethylene, ethane, propylene and propane with known composition was used for peak identification and quantification.

#### 2.5 Chemisorption and physisorption measurements

The chemisorption experiments were executed on a Quantachrome Autosorb-1C gassorption system. The sample was dried in-situ in vacuum at a temperature of 152 °C. Prior to the actual chemisorption experiment, the following pre-treatment protocol was used for the Ru catalysts. First the catalyst is reduced in H<sub>2</sub> (35 cm<sup>3</sup>/min) at 400 °C during 1 h (ramp rate 3 °C/min). After the reduction the sample was evacuated at 400 °C for 1 h and cooled in vacuum to the analysis temperature of 35 °C. The procedure is similar for the Pt and Pd catalysts but these catalysts were reduced at 300 and 200 °C, respectively. After this pre-treatment, the CO (Pd) or H<sub>2</sub> (Ru and Pt) adsorption isotherms were measured on the activated catalyst. In all steps, a temperature ramping rate of 10 °C/min and a gas flow rate of 35 cm<sup>3</sup>/min were applied. The total hydrogen adsorption isotherm was measured at room temperature up to 0.33 bar by dosing hydrogen to the sample and measuring the adsorbed amount as a function of hydrogen pressure. After adsorption, the

sample was evacuated at the same temperature for one hour and the adsorption measurement was repeated for reversible adsorption. A complete reduction of the metal surface at the pretreatment conditions and dissociative adsorption of H<sub>2</sub> on Ruthenium were used as assumptions in calculations

The BET measurements (physisorption) were performed with an ASAP 2400 (Micromeritics) gas adsorption instrument using a static volumetric adsorption and desorption method. After loading the sample, it was first evacuated at room temperature to a pressure of  $1.33 \cdot 10^{-7}$  bar or lower. Then, the evacuating temperature was raised slowly to 90 °C, avoiding a pressure raise over  $1.33 \cdot 10^{-6}$  bar. At 90 °C the sample was evacuated a few hours, at least to a pressure equal or below  $1.33 \cdot 10^{-7}$  bar. Nitrogen was used as an adsorptive gas and the measurement was done at -196 °C. The adsorption isotherm was measured by dosing nitrogen to sample (0.27 bar increments) and measuring the adsorbed amount as a function of nitrogen pressure. The measurement was continued until 98.1 % of the saturation pressure of nitrogen. The desorption isotherm was measured by decreasing the nitrogen pressure gradually, with steps of 0.04 bar. The dead volume of the system was measured with helium adsorption before the measurement.

### **3. Results and Discussion**

#### ***3.1 Selected catalysts and screening conditions***

Five noble metal catalysts (Ru/C, Ru/TiO<sub>2</sub>, Ru/Al<sub>2</sub>O<sub>3</sub>, Pt/C and Pd/C, all with 5 %-wt. active metal on support) and two typical hydrotreatment catalysts (sulphided NiMo/Al<sub>2</sub>O<sub>3</sub> and CoMo/Al<sub>2</sub>O<sub>3</sub>) were selected for these screening experiments. The noble metal catalysts were chosen because these are known to be active with respect to hydrogenation and hydrodeoxygenation [10,12,17]. Ru was selected on the basis of its high activity towards the reduction of a wide range of different oxygenates [10]. The catalytic reactions were conducted at 250 °C and 100 bar as representative conditions for mild HDO and at 350 °C and 200 bar to mimic typical deep HDO conditions. The reaction time was always 4 h, the pressure during a run was kept constant by continuous feeding of hydrogen. The reaction time was selected on the basis of earlier research performed in our group [21].

### 3.1.2 Mild HDO of pyrolysis oil

All catalytic experiments at 250 °C and 100 bar resulted in the formation of two liquid phases after reaction, a yellowish water phase and a brown oil phase with a density higher than the water phase. In addition, solids (char) were produced as well. The viscosity of the oil is a strong function of the catalyst applied. Some oils were flowable at room temperature whereas others were highly viscous and even semi-solid.

The relative amounts of the water, oil, char and gas phases were determined experimentally, allowing determination of the overall mass balance for the process. The results are presented in Figure 2. Mass balance closure varies between 77-96 %-wt. The best closures were obtained for Ru/C, Ru/TiO<sub>2</sub> and Pt/C (> 85%). The largest errors were for catalysts supported on an alumina carrier. The most likely reason for this high error is loss of product due to the very high viscosity of the upgraded pyrolysis oil obtained with this carrier. This hampers product work-up and quantification due to its tendency to stick to the reactor wall, impeller and tubing.

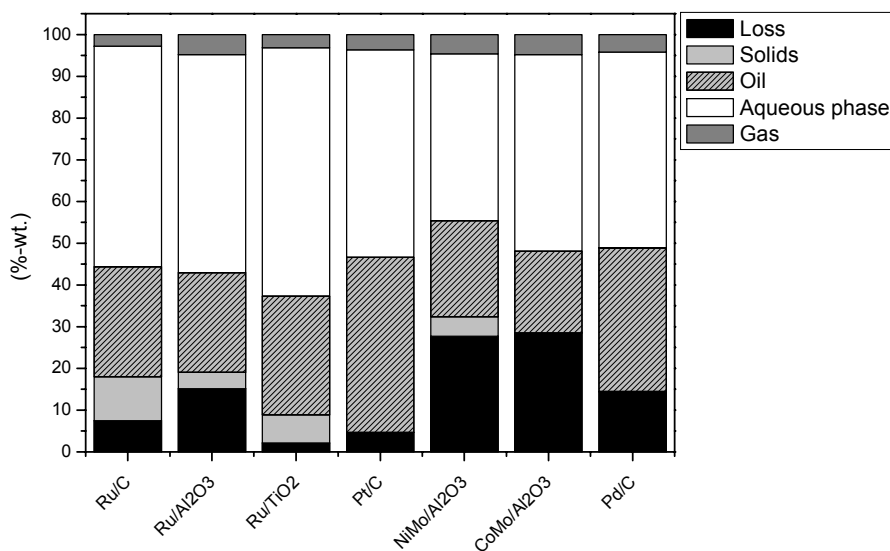


Figure 2. Mass balances for the mild HDO of pyrolysis oil with different catalysts (250 °C, 100 bar, 4 h).

The oil yield and the oxygen content of the oil (dry bases, as determined by elemental analyses) for each catalyst are depicted in Figure 3.

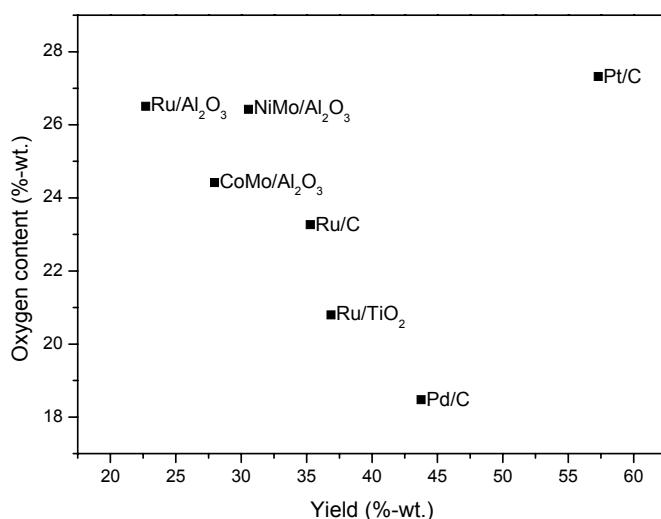


Figure 3. Oil yield and oxygen content (both on dry basis) of the oil phase from the mild HDO of pyrolysis oil (250 °C, 100 bar, 4h).

The oil yields on dry basis range between 21 and 58 %-wt. The highest yields were obtained for Pt/C, but the oil remains rich in oxygen. The yields for the sulphided CoMo and NiMo were at the low end of the range. The oxygen content of the oil phase was between 18.5 and 26.5 %-wt. The lowest value was found for the Pd/C catalyst.

When aiming at a high oil yield in combination with a low oxygen content, the Pd/C catalyst seems to be the best choice for the mild HDO process. Pt/C has the highest yield (57 %-wt.) but the oxygen content is relatively high (25 %-wt.). For comparison, the pyrolysis oil feed has an oxygen content of 42 %-wt. (dry basis). Of interest is a clear support effect for the three Ru-catalysts. With respect to both oil yield and oxygen content, TiO<sub>2</sub> and C supports perform much better than alumina. A number of explanations can be proposed to clarify these findings. It is well possible that the dispersity of the Ru particles of the various supports differs considerably, leading to different intrinsic activities [22,23]. This was indeed shown to be the case, see Table 2 for details. However, Ru on  $\gamma$ -Al<sub>2</sub>O<sub>3</sub> has the highest dispersion (22%), which is expected to be positive for catalytic activity. The relatively poor performance of the Ru on  $\gamma$ -Al<sub>2</sub>O<sub>3</sub>

catalyst is likely associated with support effect. The specific surface area of  $\gamma\text{-Al}_2\text{O}_3$  is much smaller than carbon (Table 2). Furthermore, the stability of the supports is likely to be substantially different.  $\text{TiO}_2$  and carbon are expected to be relatively inert under the conditions employed whereas  $\gamma$ -alumina is known to be susceptible by attack of acidic water at elevated conditions [23-26]. In the latter case, reaction with water leads to a reduction of the surface area due to among others crystallisation of the  $\gamma$ -alumina to a boehmite phase.

Besides the formation of two liquid phases and solids, significant amounts of gaseous components were formed as well. The amount varies between 3 %-wt. (for Ru/C) to 6 %-wt. (for Ru/ $\text{Al}_2\text{O}_3$ ). The gas phase composition after reaction was analysed and the results are given in Figure 4.

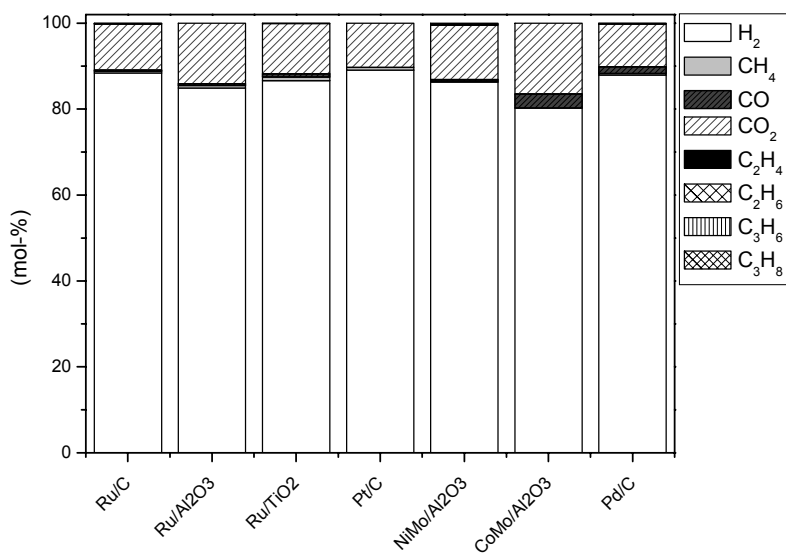


Figure 4. Gas phase composition after mild HDO of pyrolysis oil (250 °C, 100 bar, 4h) using various catalysts.

The main component is un-reacted hydrogen. Besides hydrogen,  $\text{CO}_2$  was present in amounts in between 10 and 15 %-mol. A likely pathway for the formation of  $\text{CO}_2$  is decarboxylation of organic acids. Organic acids are known to be present in pyrolysis oils in amounts varying between 1.9 and 10 %-wt. [1]. Typical examples are acetic acid and

formic acid. Decarboxylation of organic acids by the catalysts applied in this study is well established [26-28]. For CoMo, small amounts of CO were formed as well (5 %-mol), probably due to decarbonylation reactions [25,26].

### 3.1.3 Deep HDO of pyrolysis oil

Experiments aiming at a further lowering of the oxygen content (deep HDO) of pyrolysis oil were conducted at more severe conditions (350 °C and 200 bar pressure for 4 h of reaction time) than used for the mild HDO step. For the noble metal catalysts, the liquid product after reaction consisted of three different phases, a slightly yellow aqueous phase and two oil phases, one with a density higher than water and the other lower. Both product oils are miscible with each other, but apparently not with water. For the traditional hydrotreatment catalysts NiMo/Al<sub>2</sub>O<sub>3</sub> and CoMo/Al<sub>2</sub>O<sub>3</sub>, a single oil phase was produced with a density higher than the aqueous phase.

After reaction, the amounts of water, both product oils, char and gas phase were determined, allowing determination of the mass balance. Figure 5 presents the results of the mass balance calculation for the various catalysts. Mass balance closure is good and ranges between 87-100 %-wt. In line with the mild HDO experiments, the largest deviations were again observed for the catalysts on an alumina support. The HDO oils produced with these catalysts and particularly the bottom oils are highly viscous which hampers product work-up and leads to relatively high losses.

The distribution of the element carbon per phase for a typical run using Ru/C (350 °C, 200 bar, 4h) was also determined. Most of the carbon resides in both oil product phases (53.7 in the bottom and 29.2 %-wt. in the top oil). The remaining carbon resides in the solid phase (8.4 %-wt.) and gas phase (4.5 %-wt.). Also substantial amounts of carbon are present in the water phase after reaction (4.3 %-wt.), suggesting the presence of organics in the water phase. This is also supported by the acidity of the water phase (pH= 2-3), an indication for the presence of substantial amounts of organic acids. Measurement with GC-MS and 2D-GC confirmed the presence of organic acids (mainly formic acid, acetic acid) as well as alcohols (among others ethanol, propanediol) and esters (ethyl and methyl acetate).

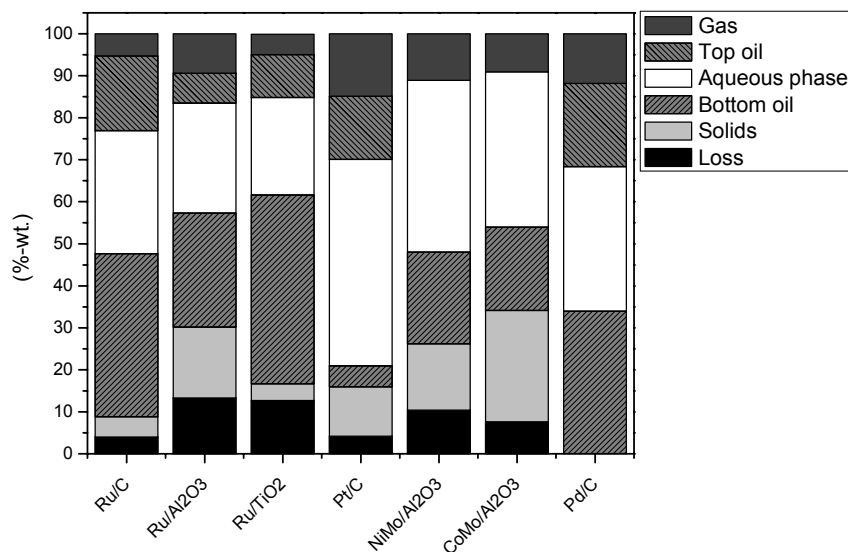


Figure 5. Mass balance for the deep HDO of pyrolysis (350 °C, 200 bar, 4h) using various catalysts.

The total product oil yield varies between 25 and 65 %-wt. (Figure 6). These yields are in the same range as reported in the literature for hydrotreating temperatures exceeding 350 °C (30-80 %-wt.), see Table 1 for details [1,2,5-8,12,15]. The highest yields were observed for Ru/TiO<sub>2</sub> and Pd/C.

The oxygen content of the various oils varies between 6 and 11 %-wt. The oxygen content is lowest for Ru/C and highest for sulphided NiMo/Al<sub>2</sub>O<sub>3</sub>. Thus, it appears that the classical sulphided hydrotreatment catalysts NiMo and CoMo on alumina are less active in the hydrotreating of pyrolysis oil to liquid organic products than noble metal catalyst. The activity and stability of these catalysts is likely reduced due to the absence of sulphur in the feed, which is known to be necessary for good catalyst performance [18,19,25,26].

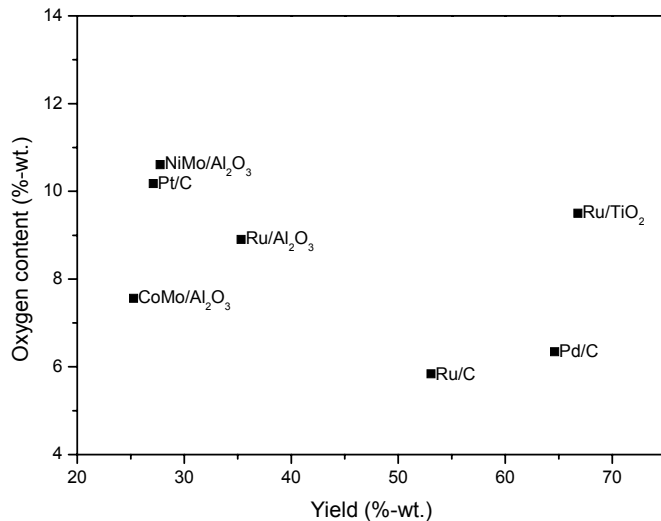


Figure 6. Oil yield and oxygen content (both on dry basis) of the combined oil phases for the deep HDO of pyrolysis oil (350 °C, 200 bar, 4 h).

The effect of the support type on the yield and deoxygenation can once more be observed for the ruthenium based catalysts. With respect to yield, the following order is observed: TiO<sub>2</sub> > C > Al<sub>2</sub>O<sub>3</sub>, with respect to deoxygenation C > Al<sub>2</sub>O<sub>3</sub> > TiO<sub>2</sub>. Thus, carbon seems the best choice when considering both oil yield and deoxygenation level. The low activity of the TiO<sub>2</sub> support may be attributed to its low surface area giving relatively large Ru particles leading to lower activity [22,23].

Besides liquid products and a char, considerable amounts of gas phase components are produced as well. The amount of gas produced varies between 6 %-wt. for Ru/C and 15 %-wt. for Pt/C (Figure 5), and implies that gasification occurs to a significant extent during the deep HDO reaction. The gas phase composition after reaction was also determined, see Figure 7 for details. For all catalysts, methane and CO<sub>2</sub> were by far the most abundant components. Large differences, though, between the catalysts were observed. For Pt/C and Pd/C all hydrogen was consumed. Apparently, hydrogen consumption for these catalysts is high (*vide infra*). When considering the relatively high H/C ratio of the product oils obtained with these catalysts (*vide infra*), it is likely that hydrogenation of e.g. C-C double bonds in addition to hydrodeoxygenation reactions also

occurs to a significant extent. This observation is confirmed by analyses of the different oil products using  $^1\text{H-NMR}$  and 2D-GC. These show an increase in the aliphatic to aromatic hydrogen ratio especially when using a Pd/C catalyst. However, particularly for Pd/C, significant amounts of methane were formed as well, which also contributes considerably to the relatively high hydrogen consumption.

Especially for the Pt and Pd catalysts, large amounts of  $\text{CO}_2$  are present in the product gas. These catalysts are known for their high decarboxylation activity for organic acids [24,27,28].

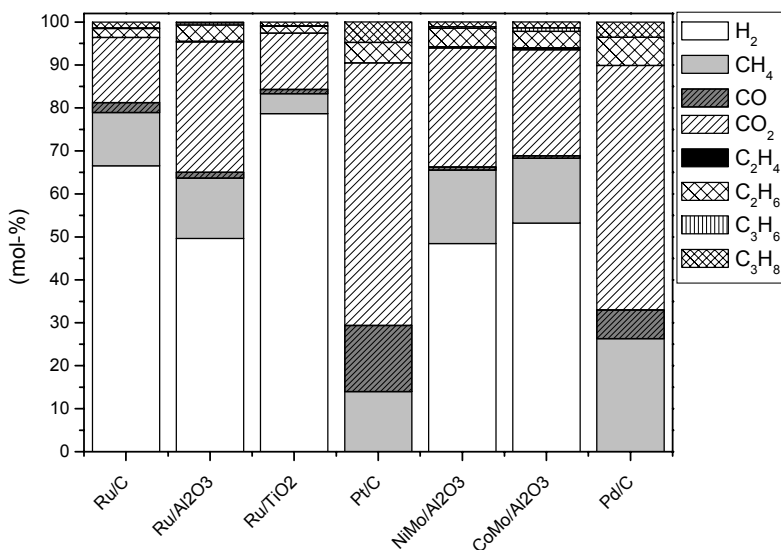


Figure 7. Gas composition for the deep HDO of pyrolysis (350 °C, 200 bar, 4h) using various catalysts.

The amount of gas produced at 350 °C and 200 bar (6 - 15 %-wt.) is considerably higher than at 250 °C and 100 bar (3-6 %-wt.). Thus gas production is more severe at higher temperatures. At 250 °C, the main gas phase component is  $\text{CO}_2$ . At more severe conditions, the amount of  $\text{CO}_2$  increases, an indication that all  $\text{CO}_2$  forming reactions are not yet complete at 250 °C and 100 bar and 4 h reaction time. In addition, considerable amounts of methane and some higher alkanes are formed (ethane and propane) at higher

temperatures. Apparently, methanation does occur at 350 °C but not yet at 250 °C [29-32].

The amount of char produced during the HDO reaction at elevated conditions varies between 4 and 26 %-wt. (see Figure 5). Very low amounts of char were observed for the carbon carriers, in particular for Pd. The catalysts on alumina support produce the highest amounts of char (26 %-wt.). This corresponds with observations reported in the literature [2,7,14,18,19], where high coke formation is shown in packed bed reactors using alumina carriers when the temperature exceeds 350 °C.

For comparison a single experiment was carried out without catalyst at 350 °C and 200 bar hydrogen (4h). The resulting product is a highly viscous tar containing suspended solids, in line with thermal deoxygenation results reported by Samolada *et al.* [15]. Thus, it may be concluded that catalysts are required to obtain low viscous, flowable oil products. The oxygen content of the tar could not be determined accurately due to the inhomogeneity of the sample. The gas phase after reaction contains about 22 %-mol of CO<sub>2</sub> indicating that CO<sub>2</sub> formation during catalytic hydrotreatment is not necessary by a catalytic pathway but may also be formed by thermal reactions.

A useful representation to gain insights in the effects of catalyst and process conditions on the elemental composition of the hydrotreated products is a van Krevelen plot [33]. The results are provided in Figure 8.

In Figure 8, two distinct areas are visible for the mild and deep HDO oils. The product oils from the deep HDO process show a lower oxygen and hydrogen content. The former is expected based on the higher anticipated deoxygenation activity at 350 °C. The H/C ratio for the product obtained at 350 °C is lower than at 250 °C. This is not anticipated at forehand, a higher hydrogenation activity is expected to lead to a higher H/C ratio. One of the possible explanations is a change in the distribution of the organics between the oil and the water phase as a function of the reaction temperature. Another possibility is the formation of re-polymerised products with a rather low H/C ratio (e.g. condensed aromatics) when performing the reaction at 350 °C. Further (analytical) studies are in progress to gain more insights in these observations.

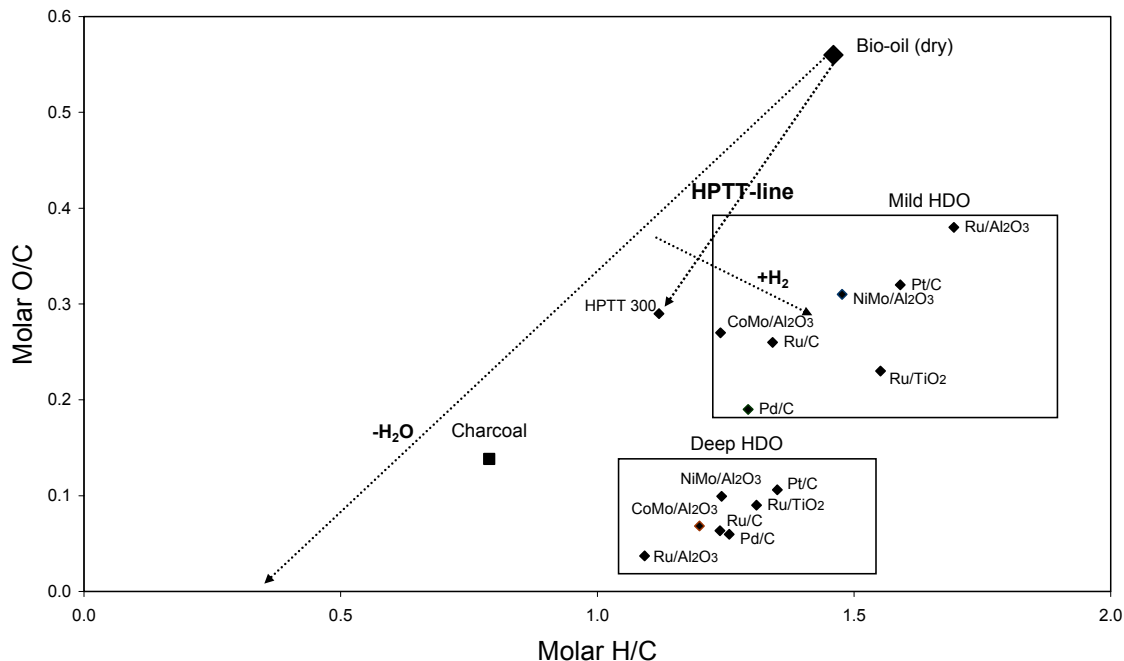


Figure 8. Van Krevelen plot for the elemental composition (dry base) of the mild and deep HDO oils using various catalysts. In the case of two oil phases, the weight average composition is used.

For comparison, the elemental composition for a typical thermally treated pyrolysis oil sample (HPTT) is also provided in Figure 8. HPTT is a process in which the pyrolysis oil is heated up to 350 °C in the absence of hydrogen at a pressure of 200 bar and a residence time of 0.5-2 min [34]. This process produces two liquid phases *viz* a water phase on top and an oil phase on the bottom which is more viscous than pyrolysis oil. During the HPTT process CO<sub>2</sub> and CH<sub>4</sub> are formed, indicative for the occurrence of thermal decarboxylation and cracking. When comparing the elemental composition of typical mild-HDO oils with that of HPTT oils, it is clear that indeed catalytic hydrotreatment occurs to a significant content.

In Figure 8 the weight averaged elemental composition of the top and bottom oil are provided for the oils obtained at 350 °C for the noble metal catalysts. It is also of interest to compare the composition of the top and bottom product phases. The results are given in Figure 9.

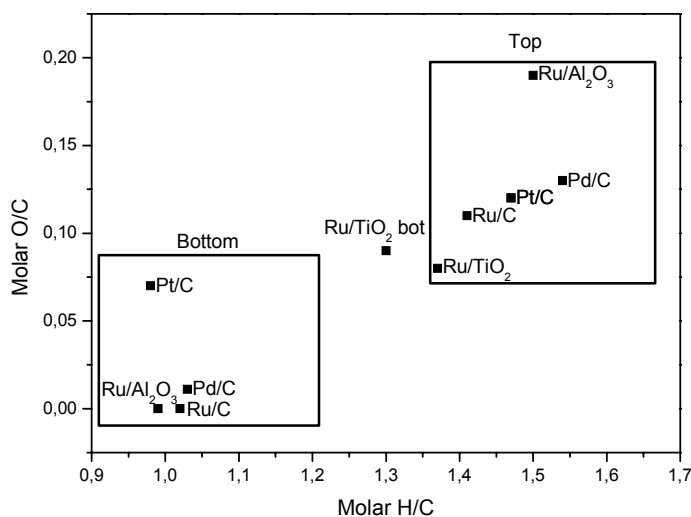
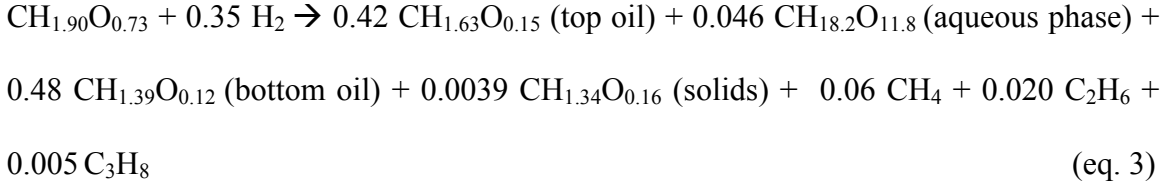
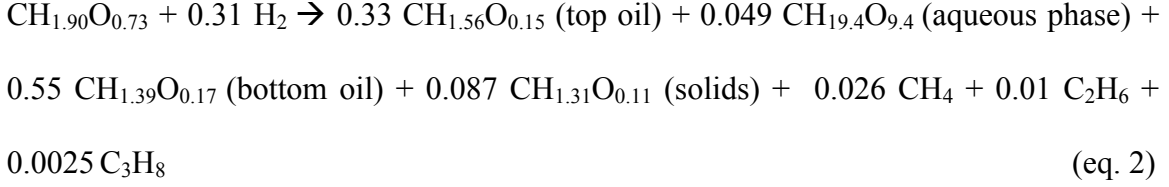


Figure 9. Van Krevelen plot for the top and bottom organic phase produced at deep HDO conditions (dry base) with various catalysts (350 °C, 200 bar, 4 h).

For all but one catalyst, the elemental composition of both the upper and bottom oil phases are within a rather narrow composition range. The exception is the bottom layer of the oil produced with Ru/TiO<sub>2</sub>. In general, the top phase has a considerably higher H/C ratio than the bottom phase, indicative for a higher aliphatic character. The O/C ratio for the top phase is slightly higher than the bottom phase, an indication that the top phase contains more oxygenates than the bottom phase.

#### 3.1.4 Hydrogen consumption for the deep HDO process

The hydrogen consumption could not be measured accurately in the experimental set-up. However, with mass balances and elemental compositions available for the various product phases, the hydrogen consumption may be calculated. Calculations were performed for the deep HDO reactions (350 °C, 200 bar, 4h) with the Ru/C and Pd/C catalysts using the reaction stoichiometry as from the elemental data of the different phases (eq. 2: Ru/C; eq. 3: Pd/C).



On basis of these data the hydrogen uptake was estimated at 400 NL/kg dry pyrolysis oil for Ru/C. As expected on the basis of the elemental composition of the oil phases and the composition of the gas phase (more CH<sub>4</sub>), the uptake for Pd/C was noticeably higher and about 450 NL H<sub>2</sub>/kg dry pyrolysis oil.

### 3.1.5 Energy distribution

With the hydrogen consumption available for two deep HDO experiments (Ru/C and Pd/C, see eq 2 and 3), the energy balance for the deep HDO using these two catalysts may be determined. This allows calculation of the energy efficiency ( $\eta$ ) of the process using equation 4. The energy efficiency give information how much of the original energy content of the original pyrolysis oil is retained in the product HDO oils. The calculations are performed on a dry basis using the higher heating values (HHV) of the various reactants/products and hydrogen usage was taken into account. The higher heating values for the pyrolysis oils and product derived thereof were calculated using Milne's formula (eq. 1), the HHV of hydrogen was taken as 141.8 MJ/kg.

$$\eta = \frac{y_{\text{HDOproduct}} \cdot \text{HHV}_{\text{HDOproduct}}}{\text{HHV}_{\text{pyrolysisoil}} + y_{\text{H}_2} \cdot \text{HHV}_{\text{H}_2}} \times 100\% \quad (\%) \quad (\text{eq. 4})$$

here  $y_{\text{HDOproduct}}$  is defined as the yield of HDO product per kg dry pyrolysis oil and  $y_{\text{H}_2}$  is the usage of hydrogen per kg dry pyrolysis oil. This yields an energy efficiency of 86 %

for Ru/C and 90 % for Pd/C. Losses are due to the formation of gas phase components, solids and residual amounts of organics in the aqueous phase.

### 3.2 Product Properties and Molecular Composition of the deep HDO oils

The desired product properties and associated molecular composition of the product oil will be application dependent. When aiming for a hydrocarbon like transportation fuel like diesel or gasoline consisting of a range of linear and cyclic hydrocarbons, the oxygenated groups in fast pyrolysis oil should be converted quantitatively. For some engines this specification might be relaxed and some oxygenates may even be preferred for better engine performance (e.g. MTBE like ethers). Clearly organic acids should be absent as these are known to have a negative effect on engine performance.

Other possible application for the hydrotreated products like co-feeding to existing refineries will require different product specification. These are expected to be depending on the feeding position in the refinery (blending with crude oil, addition in the FCC feed etc.), though exact specifications need to be developed.

The properties of the top HDO oil produced at 350 °C and 200 bar using 5 %-wt. Ru/C with a reaction time of 4h were analyzed in detail and the results are given in Table 3.

The density of the top HDO oil is 0.9 kg/l, which is lower than that of the original pyrolysis oil (1.2 kg/l) and indicates that the HDO oil is more “hydrocarbon-like”. Hydrotreatment reactions obviously lead to a large reduction in the viscosity, i.e. from 40 to 1 cP at 40 °C. These values are in line with data reported by Elliott *et al.* [9] for a HDO oil with 5 % of oxygen (2 cP at 35 °C). The acidity of the product oil is considerably lower than the original pyrolysis oil. The acidity is related to the presence of a wide variety of organic acids [1]. This reduction is due the conversion of the organic acids upon hydrotreatment, in line with the large amounts of CO<sub>2</sub> formed (*vide supra*). However, the water phase after the reaction is also acidic, meaning that part of the acids is also transferred to the water phase after reaction. The top HDO oil still contains some residual water (1.5 %-wt.) after phase separation. The oxygen content of the hydrotreated sample was 4.8 %-wt. on a dry basis, compared to 42 %-wt. for the original pyrolysis oil. As a result, the higher heating value of the product is a factor of about two higher than the pyrolysis oil feed.

Table 3. Physical properties of the fast pyrolysis oil used in this study and a representative top HDO oil (350 °C, 200 bar, 5 %-wt. Ru/C, 4h reaction time).

Property	Fast pyrolysis oil	Top HDO oil <sup>a</sup>	VGO[35]
Density (kg/l)	1.2	0.9	0.86
Viscosity (cP) at 40 °C	40	1	-
Water content (%-wt.)	30	1.5	0.1
Acidity (pH)	2.5	5.8	-
Flash point (°C)	40-65	35-39	90-180
Elemental composition, dry base (%-wt.)			
C	51.1	84.9	85.8
H	7.3	10.2	13.8
O	41.6	4.8	0.29
Higher Heating value (MJ/kg), HHV	20.3	42.6	48.9

a. prepared at 350 °C, 200 bar, 5 %-wt. Ru/C, 4h reaction time.

### 3.3.1 <sup>1</sup>H- NMR analysis of pyrolysis oil and HDO oil

<sup>1</sup>H- NMR appears a useful technique for pyrolysis oil characterization (see e.g Ingram *et al.* [36]). Important information on the amounts of various organic groups in the mixture may be obtained and pyrolysis oils from different origin and with a different processing history may be compared [36]. We have applied this classification concept for the characterization of a number of the deep HDO oils prepared in this study.

Using this concept three samples have been analysed: pyrolysis oil and two top HDO oils produced at 350 °C, 200 bar for 4 h using a Ru/C and a Pd/C catalyst. <sup>1</sup>H-NMR spectra of the fast pyrolysis oil feed and a typical HDO oil are shown in Figure 10. The functional group analysis is given in Table 4 for the samples shown in Figure 10 as well as a top oil using a Pd/C catalyst.

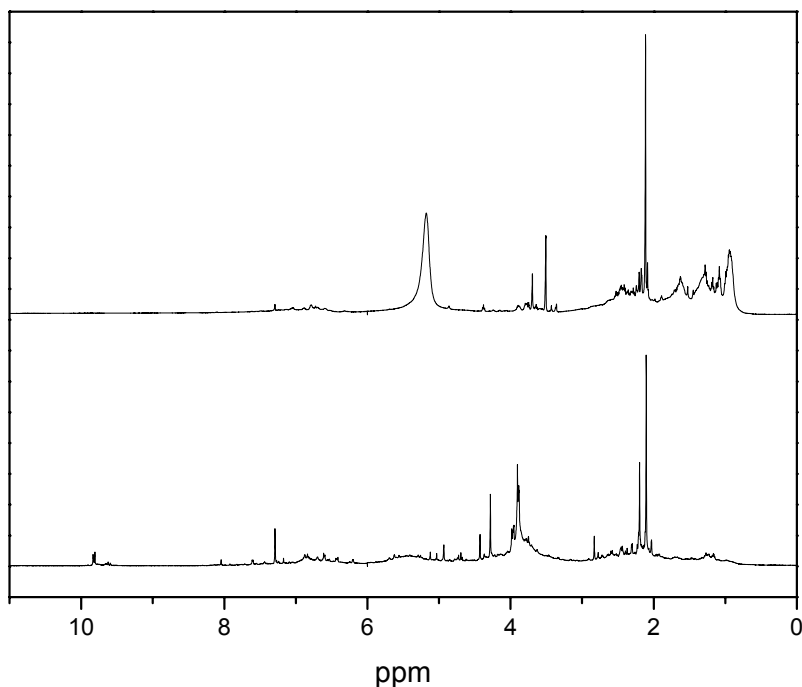


Figure 10. <sup>1</sup>H-NMR analysis of pyrolysis oil (bottom) and HDO oil (top, Ru/C, 350 °C, 200 bar, 4 h) in CDCl<sub>3</sub>.

The main differences between the two <sup>1</sup>H-NMR spectra is a strong reduction in the intensity of the peaks in the  $\delta$  3-8 ppm range and an increase of the intensity of the peaks in the  $\delta$  2.5-0.5 ppm range for the HDO oils. This is indicative for the formation of aliphatic CH<sub>2</sub> and CH<sub>3</sub> groups at the expense of oxygenates. Furthermore, the aldehyde protons (-CH(=O)) at about  $\delta$  10 ppm in the original fast pyrolysis oil are absent in the HDO oil, indicative for high aldehyde conversion during the hydrotreatment process. In addition, the intensity of the aromatic CH groups ( $\delta$  6.8-8 ppm) has reduced considerably, in line with hydrogenation of carbon-carbon double bonds to saturated aliphatics. The highest reduction in intensity was observed for the  $\delta$  4.2-3.0 ppm range. Here, characteristic resonances of methoxy groups (e.g. from lignin fragments) are present, indicative for considerable loss of these groups due to the hydrotreatment process.

Table 4. Functional group analyses of the fast pyrolysis oil used in this study and two top HDO oils using  $^1\text{H-NMR}$ .

Chemical shift region (ppm)	Type of protons	Pyrolysis oil Hydrogen content (% area of total)	Top HDO oil (Ru/C) Hydrogen content (% area of total)	Top HDO oil (Pd/C) Hydrogen content (% area of total)
10-8.0	-CHO, -COOH, downfield ArH	0.9	0	0
8.0-6.8	ArH, HC=C (conjugated)	3.3	1.4	1.3
6.8-6.4	HC=C (nonconjugated)	4.4	3.4	3.0
6.4-4.2	-CH <sub>n</sub> -O-, ArOH, HC=C (nonconjugated)	9.0	1.4	1.1
4.2-3.0	CH <sub>3</sub> O-, -CH <sub>2</sub> O-, -CHO-	26.3	6.3	2.2
3.0-2.2	CH <sub>3</sub> C(=O)-, CH <sub>3</sub> -Ar, -CH <sub>2</sub> Ar	6.4	4.9	9.5
2.2-1.6	-CH <sub>2</sub> -, aliphatic OH	32.7	16.8	9.6
1.6-0.0	-CH <sub>3</sub> -, -CH <sub>2</sub> -	17.0	64.5	73.1
Aliphatic/aromatic <sup>a</sup>	-	6.4	16.9	19.2
Atomic H/C <sup>b</sup>	-	1.69	1.41	1.54

a. Ratio of the area % at 2.2-0 ppm and 8-6.4 ppm.

b. Ratio according to the elemental composition (dry bases).

The functional group analysis also reveals interesting differences between the two top HDO oils. The aliphatic/aromatic ratio for the oil produced with Pd/C is considerably higher than that produced with Ru/C, indicating that the oil is more aliphatic in character. This is also in agreement with the elemental composition of the HDO oils, the H/C ratio for the product from the Pd/C catalyst is considerably higher (1.54) than for Ru/C (1.41).

### 3.3.2 Multidimensional GC-FID analysis of pyrolysis oil and HDO oil

Multidimensional GC has been applied to gain insights in the molecular composition of top HDO oil produced at 350 °C and 200 bar at 4h of reaction time using a Ru/C catalyst (Figure 11). In earlier work we have applied this method to classify the various component groups present in the oil [37]. The various phenolic components were divided into three subgroups, phenolics, hydroxyl-substituted acetophenones and guiacols. The three subgroups overlap in the 2D-GC chromatograms. The focus here will be on the identification and quantification of major individual components. It should be stressed here that GC techniques only provide insights in the composition of volatile components and that the higher molecular weight fraction is not analysed. The higher molecular weight fraction of raw fast pyrolysis oil may be up to 35 % [11,38,39]. For HDO oils, the amount of the non-volatile fraction is not known in detail. Thus the data provided are only for the volatile fraction and not necessary representative for the total oil.

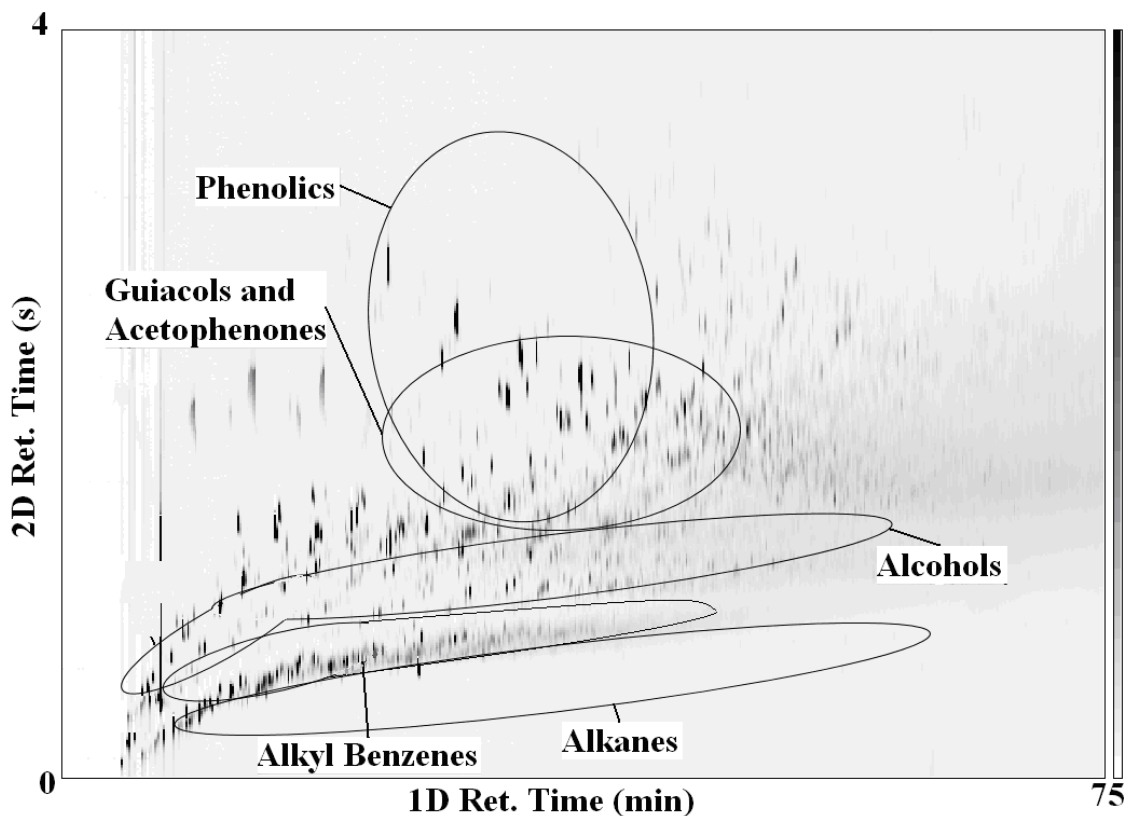
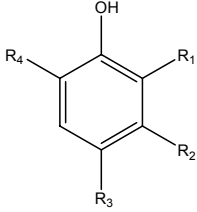
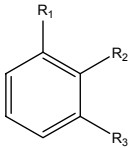
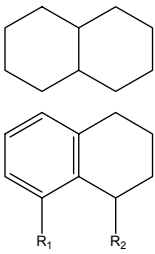
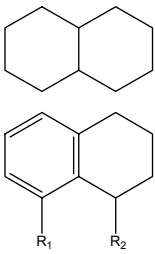


Figure 11. 2D-GC chromatogram of HDO oil produced using a Ru/C catalyst (350 °C, 200 bar, 4h).

Table 5 depicts the most abundant components classified according to component groups like phenolics, alkylbenzenes and alkanes.

Table 5. Individual compounds of selected component classes in top HDO oil produced using a Ru/C catalyst (350 °C, 200 bar)<sup>a</sup>.

Compound	Area (%)	General structure
<u>Phenolics</u>		
Phenol	0.91	
3-methylphenol	0.74	
3-Propylphenol	0.72	
4-Ethylphenol	0.74	
2-Ethyl-6-methylphenol	0.33	
2,3-dimethylphenol	0.35	
<u>Alkylbenzenes</u>		
1-methyl-2-ethylbenzene	0.35	
1,2,3-trimethylbenzene	0.11	
1-(methyl-ethyl)benzene	0.17	
<u>Naphthalenes</u>		
Decahydronaphthalene	0.11	
1,2,3,4-tetrahydro-5,7-dimethyl-naphthalene	0.09	
1,2,3,4-tetrahydro-5-methyl-naphthalene	0.08	
<u>Alkanes</u>		
Hexane	1.11	
1-ethyl-3-methylcyclopentane	0.83	
1-propylcyclopentane	0.73	
1-methylcyclohexane	0.69	
1-propylcyclohexane	0.66	
1-methyl-2-propylcyclohexane	0.66	
Heptadecane	0.49	
5-propyltridecane	0.32	
Heptane	0.32	
1,3-dimethylcyclohexane	0.30	

<sup>a</sup> R<sub>1</sub>, R<sub>2</sub>, R<sub>3</sub> and R<sub>4</sub>= H, methyl or ethyl

The phenolics are most likely products of the HDO of the lignin fraction in the original pyrolysis oil [1,38,39]. The major constituents in this group are methylated, ethylated and propylated phenolics. A variety of alkyl benzenes were also observed. These compounds are likely formed by HDO of phenolics [37-39]. Besides alkylbenzenes, partially dehydrogenated naphthalenes are also present in relative high amounts. Substantial amounts of aliphatic hydrocarbons such as linear alkanes up to C<sub>17</sub> as well as branched and cyclic derivatives were detected in the samples. These are likely formed by subsequent reactions of the phenolics and alkylbenzenes with hydrogen.

#### 4. Conclusions

A catalyst screening study using noble metal catalysts was performed on the hydrotreatment of fast pyrolysis oil. The reactions were carried out at two conditions relevant for the process, a mild hydrotreatment at 250°C (100 bar hydrogen) and a more severe hydrotreatment at 350°C (200 bar hydrogen). Distinct differences in catalyst performance, product yield and product properties were observed for mild and deep hydrotreatment.

At mild HDO conditions, a single product oil with an oxygen content between 18 and 27 %-wt. was obtained in yields between 21 and 55 %-wt. (dry basis). The yields as well as the level of deoxygenation for the noble metal catalysts were higher than for the classical hydrotreatment catalysts. At deep HDO conditions, two product liquids were obtained with the noble metal catalysts, one with a density higher and one with a density lower than water. The composition of the top oil differs from that of the bottom oil and the top oil has a higher H/C and O/C ratio. The weight average oxygen level of the product oils is between 5 and 11 %-wt., which is considerably lower than for the mild HDO process. Thus, reduction of the oxygen content below 10 %-wt. by a catalytic hydrotreatment reactions is only possible at severe conditions.

On the basis of oil yields, deoxygenation levels and hydrogen consumption, Ru/C seems the most promising catalyst for further testing in dedicated reactor set-ups. Pd/C also has potential with higher oils yields than Ru/C though with a higher product oxygen content and a larger hydrogen consumption due to enhanced methane formation.

Relevant product properties and the chemical composition of the top oil produced at deep HDO conditions (350 °C, 200 bar, 4 h) using the Ru/C catalyst were determined. The HHV is about 43 MJ/kg which is considerably higher than for the feed pyrolysis oil (20 MJ/kg). The acidity of the hydrotreated oil is considerably lower than the original feed as expressed by an increase in the pH from 2.5 to a 5.8. The molecular composition changes upon the deep HDO process were determined by 2D-GC and <sup>1</sup>H-NMR analyses on the pyrolysis feed and the product oils. Upon hydrotreatment, the aliphatic character of the oil increases (<sup>1</sup>H-NMR) which is supported by 2D-GC data showing the formation of significant amounts of phenolics, aromatics and hydrocarbons. Thus, all data imply that multiple reactions occur during the hydrotreatment process like hydrogenation, hydrogenolysis, hydrodeoxygenation, decarboxylation, decarbonylation, cracking/hydrocracking and polymerization reactions leading to the formation of coke. The application of the products derived from the deep HDO process using the noble metal catalysts may be found in the biofuels area, either (after fractionation by distillation) as a gasoline/diesel replacement or as a blend with gasoline/diesel. Engine testing in a small diesel engine with deep HDO oil produced with Ru/C catalysts have been performed and the results will be reported in in Chapter 6. The mild as well as the deep HDO products may also be useful products for co-feeding in existing oil refineries. This concept is currently receiving a great deal of attention in Europe (Biocoup) and the US [40]. The required product properties for this application will be depending on the feed location in the refinery (e.g. in the crude oil or the feed of an FCC unit) and need to be established in close collaboration with oil companies

### **Acknowledgements**

Hans van der Velde (Department of Organic Chemistry, University of Groningen) is acknowledged for performing the elemental analyses. This project was financially supported by Senter Novem (projects NEO 0268-02-03-03-0001 and DEN 2020-04-90-08-001)

## References

- [1] Bridgwater, A.; Czernik, S.; Diebold, J.; Meier, D.; Oasmaa, A.; Peacocke, C. *Fast Pyrolysis of Biomass: A handbook. Vol. 1*; CPL Press: Berkshire; 1999.
- [2] Elliott, D.C.; Schiefelbein, G.F. Liquid-Hydrocarbon Fuels from Biomass. *Abstr. Pap. Am. Chem. Soc.* **1989**, 34, 1160.
- [3] Goudriaan, F.; Peferoen, D.G.R. Liquid Fuels From Biomass via a Hydrothermal Process. *Chem. Eng. Sc.* **1990**, 45, 2729.
- [4] Grange, P.; Laurent, E.; Maggi, R.; Centeno, A.; Delmon, B. Hydrotreatment of Pyrolysis Oils from Biomass: Reactivity of the Various Categories of Oxygenated Compounds and Preliminary Techno-Economical Study. *Catal. Today.* **1996**, 29, 297.
- [5] Zhang, S.P. Study of Hydrodeoxygenation of Bio-Oil from the Fast Pyrolysis of Biomass. *Energ. Source.* **2003**, 25, 57.
- [6] Elliott, D.C. Historical Developments in Hydroprocessing of Bio-oils. *Energ. Fuel.* **2007**, 21, 1792.
- [7] Elliott, D.C.; Baker, E.G. Upgrading Biomass Liquefaction Products through Hydrodeoxygenation. *Biotechnol. Bioeng. Symp.* **1984**, suppl. 14, 159.
- [8] Baldauf, W.; Balfanz, U.; Rupp, M. Upgrading of Flash Pyrolysis Oil and Utilization in Refineries. *Biomass. Bioeng.* **1994**, 237.
- [9] Elliott D.C.; Neuenschwander, G.G. Liquid Fuels by Low-Severity Hydrotreating of Biocrude. In: Bridgwater, A.V.; Boocock, D.G.B.; editors. *Developments in Thermochemical Biomass Conversion Vol. 1*; Blackie Academic & Professional: London, 1996, 611.
- [10] Gagnon, J.; Kaliaguine, S. Catalytic Hydrotreatment of Vacuum Pyrolysis Oils from Wood. *Ind. Eng. Chem. Res.* **1988**, 27, 1783.
- [11] Oasmaa, A. Fuel Oil Quality Properties of Wood Based Pyrolysis Liquids. PhD Thesis, University of Helsinki, Helsinki, 2003.
- [12] Sheu, Y.H.E.; Anthony, R.G.; Soltes, E.J. Kinetic-Studies of Upgrading Pine Pyrolytic Oil by Hydrotreatment. *Fuel. Process. Technol.* **1988**, 19, 31.
- [13] Oasmaa, A.; Boocock, D.G.B. The Catalytic Hydrotreatment of Peat Pyrolysate Oils. *Can. J. Chem. Eng.* **1992**, 70, 294.
- [14] Conti, L.; Scano, G.; Boufala, J.; Mascia, S. Experiments of Bio-oil Hydrotreating in a Continuous Bench-Scale Plant. In: Bridgwater, A.V.; Hogan, E.N., editors. *Bio-Oil Production and Utilization*. CPL Press, Newbury Berks, 1996, 198.

- [15] Samolada, M.C.; Baldauf, W.; Vasalos, I.A. Production of a Bio-Gasoline by Upgrading Biomass Flash Pyrolysis Liquids via Hydrogen Processing and Catalytic Cracking. *Fuel*. **1998**, 77, 1667.
- [16] Elliott, D.C.; Neuenschwander, G.G.; Hart, T.R.; Hu, J.; Solana, A.E.; Cao, C. Hydrogenation of Bio-Oil for Chemical and Fuel Production. In: Bridgwater, A.V.; Boocock, D.G.B., editors. *Science in Thermal and Chemical Biomass Conversion*. CPL Press: Newbury Berks, 2006, 1536.
- [17] Elliott, D.C.; Peterson, K.L.; Muzatko, D.S.; Alderson, E.V.; Hart, T.R.; Neuenschwander, G.G. Effects of Trace Contaminants on Catalytic Processing of Biomass-Derived Feedstocks. *Appl. Biochem. Biotech.* **2004**, 113, 807.
- [18] Furimsky, E. Catalytic Hydrodeoxygenation. *Appl. Catal. A-gen.* 2000, 199, 147.
- [19] Furimsky, E.; Massoth, F.E. Deactivation of Hydroprocessing Catalysts. *Catal. Today*. 1999, 52, 381.
- [20] Milne, T. A.; Brennan, A. H.; Glenn, B. H. *Source Book of Methods of Analysis for Biomass and Biomass Conversion Processes*. Elsevier Applied Science: London, 1990.
- [21] Mahfud, F. Exploratory Studies on Fast Pyrolysis Oil Upgrading. PhD thesis, University of Groningen, Groningen, **2007**.
- [22] Osada, M.; Sato, O.; Arai, K.; Shirai, M. Stability of Supported Ruthenium Catalysts for Lignin Gasification in Supercritical Water. *Energ. Fuel*. **2006**, 20, 2337.
- [23] Elliott, D. C.; Sealock, L. J.; Baker E. G. Chemical Processing in High Pressure Aqueous Environments. 2. Development of Catalysts for Gasification. *Ind. Eng. Chem. Res.* **1993**, 32, 1542.
- [24] Eilos, I.; Pyhälähti, A.; Nurminen, M.; Puroola, V. Proces for the Hydrogenation of Olefins. 7473811, 2005.
- [25] Laurent, E.; Delmon, B. Influence of Oxygen-Containing, Nitrogen-Containing, and Sulfur-Containing-Compounds on the Hydrodeoxygenation of Phenols over Sulphided  $\text{Co}/\text{Al}_2\text{O}_3$  and  $\text{NiMo}/\text{Al}_2\text{O}_3$  Catalysts. *Ind. Eng. Chem. Res.* **1993**, 32, 2516.
- [26] Laurent, E.; Delmon, B. Influence of Water in the Deactivation of a Sulphided  $\text{NiMo}/\gamma\text{-Al}_2\text{O}_3$  Catalyst during Hydrodeoxygenation. *J. Catal.* **1994**, 146, 281.
- [27] Masende, Z.P.F.; Kuster, B.F.M.; Ptasinski, K.J.; Janssen, F.J.J.G; Katima, J.H.Y.; Schouten, J.C. Kinetics of Malonic Acid Degradation in Aqueous Phase over a Pt/Graphite Catalyst. *Appl. Catal. B-Env.* **2005**, 56, 189.

- [28] Kubickova, I.; Snare, M.; Eranen, K.; Maki-Arvela, P.; Murzin, D.Y. Hydrocarbons for Diesel via Decarboxylation of Vegetable Oils. *Catal. Today*. **2005**, 106, 197.
- [29] Brooks, K. P.; Hu, J. L.; Zhu, H. Y.; Kee, R. J. Methanation of Carbon Dioxide by Hydrogen Reduction using the Sabatier Process in Microchannel Reactors. *Chem. Eng. Sci.* **2007**, 62, 1161.
- [30] Elliott, D. J.; Lunsford, J. H. Kinetics of the Methanation Reaction over Ru, Ru-Ni, Ru-Cu, and Ni Clusters in Zeolite-y. *J. Catal.* **1979**, 57, 11.
- [31] Weatherbee, G.D.; Bartholomew, C.H. Hydrogenation of CO<sub>2</sub> on Group-VIII Metals. 2. Kinetics and Mechanism of CO<sub>2</sub> Hydrogenation on Nickel. *J. Catal.* **1982**, 77, 460.
- [32] Winslow, P.; Bell, A.T. Studies of Carbon-Containing and Hydrogen-Containing Adspecies present during CO Hydrogenation over Unsupported Ru Ni and Rh. *J. Catal.* **1985**, 94, 385.
- [33] Van Krevelen, D. W. Graphical Statistical Method for the Study of Structure and Reaction Processes of Coal. *Fuel*. **1950**, 29, 269.
- [34] Venderbosch, R. H.; Sander, C.; Tjeerdsma, B. *Hydrothermal Conversion of Wet Biomass*. Utrecht, **1999**, Gave Report 9919, Novem.
- [35] Soskind, D.M., Samoilova, N.N., Voronova, O.K., Shabalina, T.N. Kuznetsova, N.N., Catalytic Cracking of Vacuum Gasoil from Mangyshlak Crude on Zeolitic Catalysts. *Chem. Tech Fuels. Oil*. **1980**, 16, 10.
- [36] Ingram, L.; Mohan, D.; Bricka, M.; Steele, P.; Strobel, D.; Crocker, D.; Mitchell, B.; Mohammed, J.; Cantrell, K.; Pittman, C.U. Pyrolysis of Wood and Bark in an Auger Reactor: Physical Properties and Chemical Analysis of the Produced Bio-Oils. *Energ. Fuel*. **2008**, 22, 614.
- [37] Marsman, J.H.; Wildschut, J.; Mahfud, F.H.; Heeres, H.J. Identification of Components in Fast Pyrolysis Oil and Upgraded Products by Comprehensive Two-Dimensional Gas Chromatography and Flame Ionisation Detection. *J. Chrom. A*. **2007**, 1150, 21.
- [38] Oasmaa, A.; Kuoppala, E.; Gust, S.; Solantausta, Y. Fast Pyrolysis of Forestry Residue. 1. Effect of Extractives on Phase Separation of Pyrolysis Liquids. *Energ. Fuel*. **2003**, 17, 1.
- [39] Oasmaa, A.; Kuoppala, E.; Solantausta, Y. Fast Pyrolysis of Forestry Residue. 2. Physicochemical Composition of Product Liquid. *Energ. Fuel*. **2003**, 17, 433.
- [40] Internet: <http://www.biocoup.com>

